ACS APPLIED MATERIALS & INTERFACES

Research Article

www.acsami.org

# Design, Fabrication, and Characterization of Archaeal Tetraether Free-Standing Planar Membranes in a PDMS- and PCB-Based Fluidic Platform

Xiang Ren,[†] Kewei Liu,[†] Qingwei Zhang,[†] Hongseok "Moses" Noh,[†] E. Caglan Kumbur,[†] Wenqiao Wayne Yuan,[‡] Jack G. Zhou,*[,†] and Parkson Lee-Gau Chong*[,§]

[†]Department of Mechanical Engineering and Mechanics, Drexel University, Philadelphia, Pennsylvania 19104, United States

[‡]Department of Biological and Agricultural Engineering, North Carolina State University, Raleigh, North Carolina 27695, United States

[§]Department of Biochemistry, Temple University School of Medicine, Philadelphia, Pennsylvania 19140, United States

Supporting Information

**ABSTRACT:** The polar lipid fraction E (PLFE) isolated from the thermoacidophilic archaeon *Sulfolobus acidocaldarius* contains exclusively bipolar tetraether lipids, which are able to form extraordinarily stable vesicular membranes against a number of chemical, physical, and mechanical stressors. PLFE liposomes have thus been considered appealing biomaterials holding great promise for biotechnology applications such as drug delivery and biosensing. Here we demonstrated that PLFE can also form free-standing "planar" membranes on micropores (~100 μm) of polydimethylsiloxane (PDMS) thin films embedded in printed circuit board (PCB)-based fluidics. To build this device, two novel approaches were employed: (i) an S1813 sacrificial layer was used to facilitate the fabrication of the PDMS thin film, and (ii) oxygen plasma treatment was utilized to conveniently bond the PDMS thin film to the PCB board and the PDMS fluidic chamber. Using electrochemical impedance spectroscopy, we found that the dielectric properties of PLFE planar membranes suspended on the PDMS films are distinctly different from those obtained from diester lipid and triblock copolymer membranes. In addition to resistance (R) and capacitance (C) that were commonly seen in all the membranes examined, PLFE planar membranes showed an inductance (L) component. Furthermore, PLFE planar membranes displayed a relatively large membrane resistance, suggesting that, among the membranes examined, PLFE planar membrane would be a better matrix for studying channel proteins and transmembrane events. PLFE planar membranes also exhibited a sharp decrease in phase angle with the frequency of the input AC signal at ~1 MHz, which could be utilized to develop sensors for monitoring PLFE membrane integrity in fluidics. Since the stability of free-standing planar lipid membranes increases with increasing membrane packing tightness and PLFE lipid membranes are more tightly packed than those made of diester lipids, PLFE free-standing planar membranes are expected to be considerably stable. All these salient features make PLFE planar membranes particularly attractive for model studies of channel proteins and transmembrane events and for high-throughput drug screening and artificial photosynthesis. This work can be extended to nanopores of PDMS thin films in microfluidics and eventually aid in membrane-based new lab-on-a-chip applications.

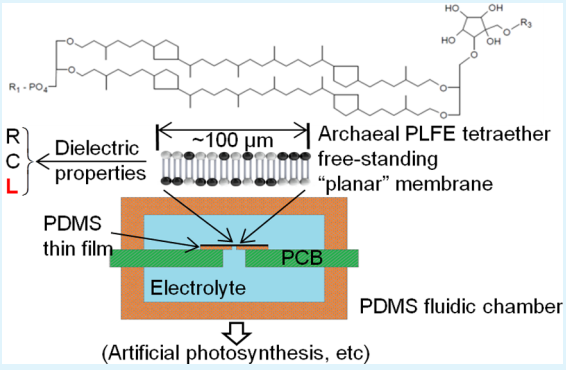


**KEYWORDS:** *archaeal bipolar tetraether lipids, free-standing planar membranes, fluidics, PDMS film, electrochemical impedance spectroscopy*

## 1. INTRODUCTION

Fluidic devices containing lipid or polymer membranes have a wide range of biotechnology applications such as ion channel recording, high-throughput drug screening, and artificial photosynthesis.[1−4] Both vesicular membranes and free-standing planar membranes have been built into fluidics for prototype studies of membrane channel proteins and membrane transport processes. Vesicular membranes are relatively more stable, more facile to fabricate, and easier to incorporate into fluidic devices than free-standing planar membranes. For example, triblock copolymer vesicular membranes[5] containing the membrane-bound proteins, namely, bacteriorhodopsin (BR) and ATP synthase, have been incorporated into a foam architecture as an artificial photosynthesis fluidic system.[2,3] BR absorbs green light and uses the light

Received: April 29, 2014
Accepted: June 17, 2014
Published: June 17, 2014

  

energy to pump protons across vesicular membranes. The proton gradient then activates ATP synthase, which converts adenosine diphosphate and monophosphate to adenosine triphosphate (ATP).[3,6] ATP can be subsequently engineered to generate biofuels.[7]

Compared to vesicular membranes, free-standing planar membranes are less stable. Traditional free-standing lipid membranes (black lipid membranes), which suspend a pinhole of the size ~0.1−1.0 mm on Teflon or silicon support, are prone to mechanical distortion and become ruptured easily in one single event leading to the loss of membrane electrical resistance in a few minutes to several hours.[8−10] Membrane stability was improved when free-standing membrane was formed on a porous alumina or silicon nitride membrane substrate with an array of nanosize pores.[11,12] In such nanoblack lipid membrane systems, each single membrane covering a pore ruptures in a stochastic manner leading to a continuous decrease in overall membrane resistance over a period of days.[11,12] The stability of the suspended lipid bilayers depends on membrane composition and increases with decreasing pore size and with increasing molecular order of the lipids.[1,12,13]

Despite that the stability issue remains unsettled, free-standing planar membranes on pore support offer some key advantages for fluidics applications: (i) both sides of the membrane are readily accessible for studies of membrane channel proteins and membrane transport processes, (ii) the electrolyte on either side can be conveniently replaced or adjusted, (iii) there is no complication in experiments or data interpretation due to vesicle aggregation or fusion, and (iv) the membrane can be applied to chip technology, especially for the establishment of biosensing and high-throughput screening assays. Therefore, it is of interest to develop a new free-standing planar membrane system on nano- or micropores with much improved membrane stability.

In the present study, our membrane design involved the use of archaeal bipolar tetraether lipids. Specifically, we used the polar lipid fraction E (PLFE) isolated from the thermoacidophilic archaeon *Sulfolobus acidocaldarius* (optimum growth: 80 °C and pH 2−3)[14] to make free-standing planar membrane on the micropores of the polydimethylsiloxane (PDMS) films. PLFE bipolar tetraether lipids are appealing biomaterials and structurally distinctly different from diester lipids found in mammalians or bacteria.[15,16] PLFE is a mixture of calditolglycerocaldarchaeol (also termed glycerol dialkylcalditol tetraether, GDNT) and caldarchaeol (also termed glycerol dialkylglycerol tetraether, GDGT)[17,18] (Supporting Information Figure S1). The GDNT component (~90% of total PLFE) contains phospho-*myo*-inositol on the glycerol end and $\beta$-glucose on the calditol end, whereas the GDGT component (~10% of total PLFE) has phospho-*myo*-inositol attached to one glycerol and $\beta$-D-galactosyl-D-glucose to the other glycerol skeleton. The nonpolar regions of these lipids consist of a pair of 40-carbon biphytanyl chains, each of which contains up to four cyclopentane rings. The tetraether linkages, the cyclopentane rings, and the lack of C═C bonds in the biphytanyl chains make PLFE lipids chemically much more stable than diester lipids.

PLFE lipids are able to form vesicles of varying sizes and supported monolayers in the air−water interface.[19,20] The *d*-spacing of PLFE lipid membrane is ~4.9 nm at room temperature (~22 °C) as revealed by small-angle X-ray scattering.[21] PLFE lipid membranes (in either vesicle or supported monolayer form) are extraordinarily stable against chemical, physical, and mechanical stressors (e.g., pH, detergents, pro-oxidants, fusogenic compounds, certain phospholipases, pressure, and temperature) (reviewed in refs 15,22). The extraordinary stability of PLFE liposomes can be attributed to the tight and rigid membrane packing due to the presence of tetraether linkages and cyclopentane rings in the bidiphytanyl chains as well as an extensive network of hydrogen bonds created by the sugar and phosphate residues exposed at the outer face of tetraether liposomes (reviewed in refs 15,22−24). This unusually tight and rigid membrane packing in PLFE liposomes is mostly manifested in the data of volume fluctuations, which are exceedingly low, as compared to those of dipalmitoyl-*sn*-glycero-3-phosphocholine (DPPC, a diester lipid) bilayers, over a wide range of temperatures.[25] To our knowledge, free-standing PLFE planar lipid membranes have not been reported in the literature. Since it is known that the stability of free-standing planar lipid membranes increases with increasing membrane packing tightness[1] and since PLFE liposomal membranes are more tightly packed than other liposomes, PLFE free-standing planar membranes are expected to be much more stable than those made of diester lipids. Thus, the use of PLFE would alleviate the stability problem of free-standing lipid membranes mentioned earlier.

In this paper, we report the design, fabrication, and characterization of PLFE free-standing lipid membranes situated on micropores of a PDMS thin film embedded in a printed circuit board (PCB)-based fluidic device. In order to fabricate a large number of uniformly produced micrometer-sized pinholes on PDMS thin films, we developed a new micro molding method involving oxygen plasma treatment of SU-8 (an epoxy-based negative photoresist polymer) and the use of the positive photoresist polymer S1813 as a dissolvable sacrificial layer between the SU-8 mold and the PDMS thin film. We also used electrochemical impedance spectroscopy (EIS) to demonstrate that PLFE lipids can form free-standing planar membranes over the micropores of PDMS thin films. In addition, we used EIS to compare the dielectric properties of PLFE free-standing planar lipid membranes with those obtained from diester lipid membranes (e.g., 1-palmitoyl-2-oleoyl-*sn*-glycero-3-phosphocholine (POPC) and POPC/1-palmitoyl-2-oleoyl-*sn*-glycero-3-phosphoserine (POPS)) or triblock copolymer (e.g., poly(2-methyloxazoline)-*block*-poly(dimethylsiloxane)-*block*-poly(2-methyloxazoline) (PMOXA-PDMS-PMOXA)) membranes. Moreover, throughout this paper, the potential application of the PLFE free-standing planar membrane-based fluidics in artificial photosynthesis is discussed.

## 2. EXPERIMENTAL SECTION

**2.1. Triblock Copolymer.** Triblock copolymer PMOXA-PDMS-PMOXA (SI Figure S2; MW = 1300−8500−1300 g/mol) was purchased from Polymer Source (Quebec, Canada). It contains a hydrophobic layer (dimethylsiloxane) set between two hydrophilic layers (methyloxazoline). Like many other amphiphilic molecules, triblock copolymer can form micelles, vesicles, or planar membranes in aqueous solution.[26] PMOXA-PDMS-PMOXA was dissolved in chloroform (2 wt %) as the stock solution and diluted to 1 wt % with toluene prior to use.[6]

**2.2. Lipids.** POPC and POPS were purchased from Avanti Polar Lipids (Alabaster, AL). These two diester lipids (SI Figure S2) are commonly seen in mammalian or bacterial cells. PLFE bipolar tetraether lipids (SI Figure S1) were isolated from *S. acidocaldarius* as previously described.[14] POPC and POPS stock solutions were made in chloroform. PLFE stock solution was made using a mixture of chloroform:methanol:water (14:5:1, v/v/v).

**2.3. Selection of PDMS.** PDMS is known to promote the formation of free-standing membranes over pinholes due to its ability to conduct spontaneous organic solvent extraction.[1] PDMS can be easily molded on

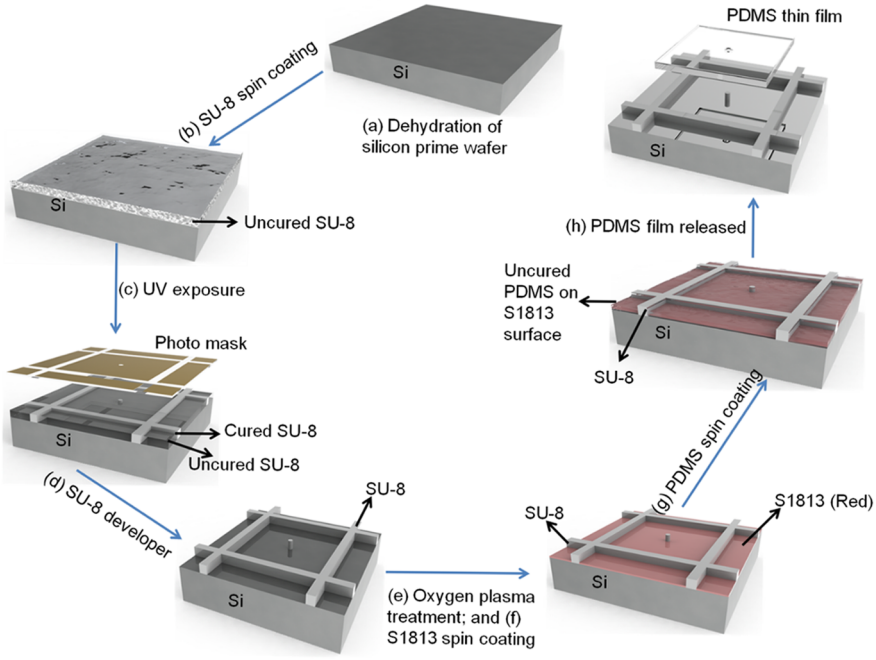


**Figure 1.** PDMS thin film fabrication procedures.

both macro and micro scales.[27] Additionally, PDMS is optically transparent, which is desirable for certain applications such as artificial photosynthesis. For these reasons, PDMS was chosen as the material to make both fluidic chambers and thin films holding free-standing membranes. We used Sylgard 184 kit (Dow Corning, Midland, MI) to prepare PDMS.

**2.4. Fabrication of PDMS Thin Film.** The PDMS thin film with pinholes for supporting triblock copolymer or lipid membranes was fabricated in a cleanroom. The fabrication process is described as follows (Figure 1):

(a) Cleaning and dehydration of silicon wafer: A prime-grade 4 in. silicon wafer was cleaned and dehydrated on a hot plate at 110 °C for 5 min.

(b) SU-8 spin coating: Negative photoresist SU-8 2035 (MicroChem, Newton, MA) was chosen as the molding material. The SU-8 2035 was spin-coated on the silicon wafer at 500 rpm (revolutions per minute) with an acceleration of 100 r/s for 30 s using a photoresist spinner (CEE, model 100, Rolla, MO). This resulted in an uncured SU-8 layer with a thickness of ∼200 $\mu$m. The wafer was then soft-baked on a hot plate at 65 °C for 15 min followed by heating at 95 °C for 60 min and slow cooling to room temperature.

(c) UV exposure: The wafer with an uncured SU-8 layer was moved to a mask aligner (model 206, OAI, San Jose, CA; UV intensity: 23.1 mW/cm$^2$; wavelength: 365 nm). The SU-8 layer was a negative mask with multiple blank holes to make standing bars for molding the PDMS thin film holes. The total energy required for SU-8 molding was 500 mJ/cm$^2$; therefore, the exposure time was set to 21.7 s at 23.1 mW/cm$^2$.[28] After the UV exposure, the wafer was placed onto a hot plate baked at 65 °C for 10 min and then at 95 °C for 30 min. Postexposure bake was necessary in order to convert the UV exposed areas to the cured SU-8 (a cross-linked solid structure).

(d) SU-8 developer: When the wafer was cooled down again, it was immersed into a SU-8 developer (MicroChem, Newton, MA) for 10 min to remove the uncured SU-8. This was followed by rinsing first with isopropanol and then deionized water. Finally, the wafer was dried with nitrogen, and a SU-8 mold for the PDMS film was fabricated.

(e) Oxygen plasma treatment of the SU-8 mold: The PDMS thin film with holes would be too thin and fragile to be peeled off from the SU-8 mold. To solve this problem, we used the positive photoresist S1813 (Shipley 1813, MicroChem, Newton, MA) to build a dissolvable sacrificial layer between the SU-8 mold and the PDMS thin film. Before coating the S1813 thin layer, oxygen plasma treatment of the SU-8 surface was performed on a plasma cleaner (model COVANCE, FEMTO Science, Hwaseong-si, Gyeonggi, South Korea) using 110 V AC and 50 Hz. Oxygen plasma treatment makes the SU-8 surface more hydrophilic[29] to suit for coating with S1813.

(f) S1813 sacrificial layer spin coating: After oxygen plasma treatment, positive photoresist S1813 was dispensed onto the center of the cured SU-8 structure. Spinning coating was set at 2500 rpm with an acceleration of 1000 r/s for 60 s. Then, the wafer was hard-baked on a hot plate at 120 °C for 5 min. This results in a ∼4−6 $\mu$m S1813 layer on SU-8.

(g) Formation of PDMS thin film: The PDMS prepolymer (SYLGARD 184 silicone elastomer, Dow Corning, Midland, MI) and PDMS curing agent (SYLGARD 184 silicone elastomer curing agent, Dow Corning) were thoroughly mixed at a weight ratio of 10:1 to form the PDMS mixture. The mixture was placed in a vacuum desiccator for 30 min to fully remove the air bubbles. The PDMS mixture was poured slowly onto the center of the S1813/SU-8-coated silicon wafer. Spinning coating was performed at 1500 rpm with an acceleration rate 500 r/s for 60 s, which resulted in a PDMS thin film (thickness ∼80−120 $\mu$m) with an array of small holes. The wafer with PDMS was then placed in a 60 °C oven for 24 h to allow the PDMS thin film to be cured and solidified.

(h) PDMS film release: The positive photoresist S1813 layer between the silicon wafer and PDMS film was dissolved by acetone. The released PDMS film with multiple pinholes was further cleaned using isopropanol. This method provides an effective way to peel off thin PDMS films from the mold without breaking any micro structure. The resulting PDMS film was cut into multiple single units, each of which contains only one single aperture (diameter: 0.1 or 0.2 mm). For the sake of clarity, Figure 1 shows only the fabrication of one single unit.

**2.5. Fabrication of PDMS Fluidic Devices.** The fluidic device was also made of PDMS. We designed the 3D structures as the mold of a PDMS fluidic device (Figure 2) and then exported them using a stereolithography machine (EnvisionTEC, model Perfactory, Gladbeck, Germany; voxel resolution: 35 $\mu$m). Photosensitive polymer Photosilver (EnvisionTEC) was used to make the mold of the entire fluidic device (Figure 2). The PDMS mixture (described in Section 2.4(g)) was poured onto the Photosilver mold and degassed under vacuum for 1 h. The PDMS/Photosilver mold was incubated at 60 °C for 24 h to allow the PDMS to be cured and solidified. The resulting PDMS chamber can be easily peeled off from the Photosilver mold.

**2.6. PCB Board and Electrodes.** The PCB board was designed using the PCB layout software (PCB Artist) and fabricated by Advanced

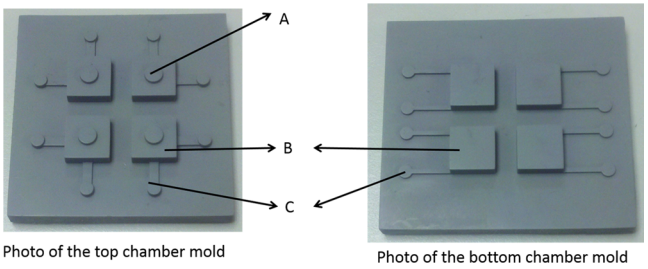


**Figure 2.** 3D lithography of the PDMS chamber mold made by a photopolymer Photosilver. Each mold contains four identical chamber units (B). The center of each chamber unit contains a reserved window for further applications (for example, allowing green light to go through in order to elicit the light reaction in artificial photosynthesis) (A). There are microchannels with inlets and outlets (C) associated with each chamber unit.

Circuits (Tempe, AZ). The PCB board contained two electrodes for impedance measurements of the planar membrane. The electrode surface was copper coated with nickel. In the absence of inert metals such as gold and nickel, a copper electrode would be dissolved in the buffer solution during long-term use if a dc current was continuously applied.

**2.7. Assembly of PDMS Fluidic Chambers, PCB Board, and PDMS Thin Films with Planar Lipid or Copolymer Membranes.** Oxygen plasma treatment method was used to bond the PCB board to the PDMS thin films and the PDMS fluidic chambers.[30] Oxygen plasma can turn some of the methyl groups on PDMS surface into hydroxyl groups, which are more hydrophilic and capable of bonding with other plasma-treated PDMS or PCB surfaces.[31]

Figure 3 describes how the fluidics device is assembled. (1) The bottom part of the PDMS chamber and the PCB board were cleaned, put in the plasma generator, and treated with oxygen plasma for 70 s. Then, the PCB board and the PDMS bottom chamber were compressed together for 1 min to have these two components strongly bonded. (2) Oxygen plasma treatment was also applied to the PDMS thin film (5 mm × 5 mm × 100 $\mu$m), which was bonded to the PCB board. (3) Electrolyte was introduced to the PDMS chamber, followed by the deposit of lipids or copolymer to generate planar membranes over the microhole on the PDMS thin film (see Section 2.8). (4) The PDMS top chamber (pretreated with oxygen plasma) was bonded to the PCB board and filled with electrolyte. Figure 4 shows the image of the assembled PCB-based fluidic device. Each PCB board contains four identical PDMS chambers.

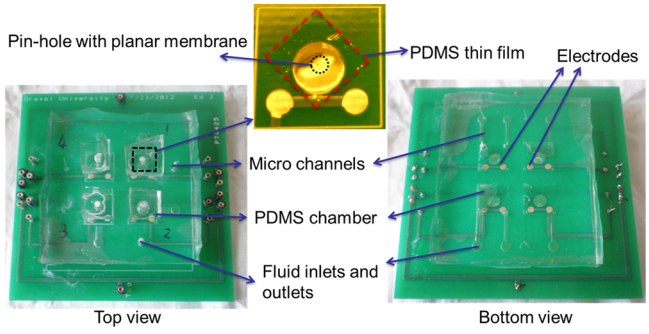


**Figure 4.** Image of the assembled PCB-based fluidic device.

These procedures provided a fast, clean, and convenient bonding method for linking the PCB board to the PDMS thin film or to the PDMS fluidic device. Even though oxygen plasma treatment did not create a permanent bonding, it could last for over 2 weeks, long enough for the electrochemical measurements which usually take several hours. Both PCB and PDMS surface can be hydroxylized by oxygen plasma treatment (as illustrated[31]), which makes the surface more hydrophilic. Other than this chemical modification on the surface, we are not aware of oxygen plasma treatment introducing any significant chemical impurity to the PCB board or PDMS fluidic device (i.e., PDMS chamber). In this regard, oxygen plasma treatment was better than some other bonding methods such as the use of glues.[32]

**2.8. Formation of Planar Membranes.** Assembly b shown in Figure 3 was placed on the bottom of a 6 in. Petri dish and submerged in 10 mM Tris (tris(hydroxymethyl)aminomethane) buffer (pH 7.4) containing 1 M KCl and 1 mM $CaCl_2$.[33] Then, a droplet of the triblock copolymer or lipid stock solution was added to the buffer layer. Copolymer or lipid molecules presumably spread over the aqueous surface layer, and when the PDMS thin film was lifted up, polymers or lipids that were near the aperture spontaneously aggregate to form a free-standing planar membrane over the aperture. It is known that diester lipids can form free-standing planar membranes on pinholes in PDMS thin film, silicon dioxide, or other semiconductor materials.[34,35] In this study, we demonstrated that PLFE archaeal tetraether lipids can

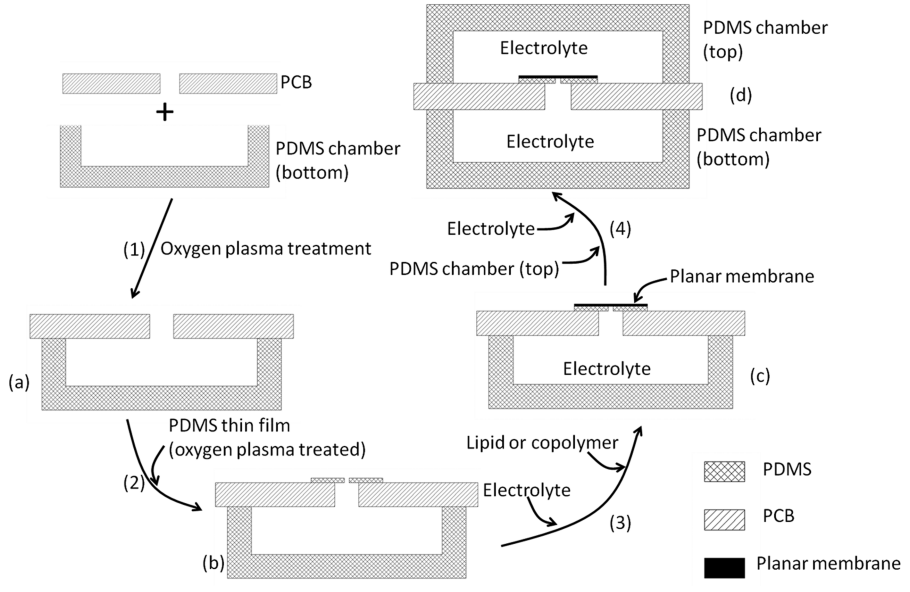


**Figure 3.** Procedures for assembling the fluidics device.

also form free-standing "planar" membranes on pinholes in PDMS thin films.

**2.9. Impedance Measurements.** In each PDMS chamber (Assembly d in Figure 3) of the fabricated fluidic PCB board, the PDMS thin film separates the chamber into two compartments, each of which contains an electrode connected to an external circuit as conceptually illustrated in Figure 5. The electrochemical impedance spectroscopic measurements were performed on a Bio-Logic SAS instrument (model VSP, Claix, France) at room temperature (~22 °C) in the same Tris buffer as described.[33,36] The frequency of the AC input signal from the instrument varied from 1 MHz to 10 mHz, and the input signal had a voltage peak of 100 mV (from zero voltage to the peak of the sine wave). In each frequency decade, six sets of voltage and current data were collected. The data acquisition software was able to automatically calculate a fit curve and generate an equivalent circuit with detailed value of each component, such as resistance $R$, capacitance $C$, and inductance $L$. The circuit parameters could provide the information about the real and imaginary value of the sample's impedance properties. The data were analyzed and plotted using Matlab.

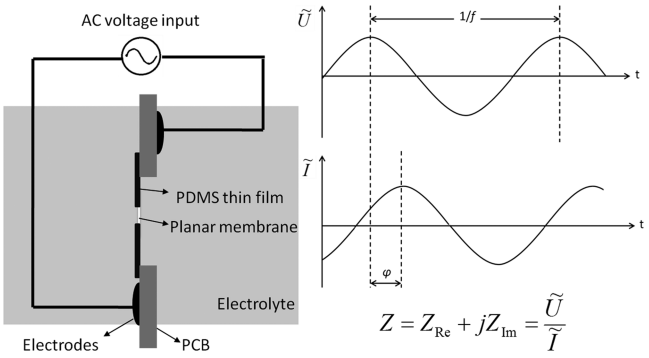


**Figure 5.** Conceptual illustration of the electrochemical impedance spectroscopy setup for a planar membrane on a PDMS thin film sitting on the PCB board within a PDMS chamber. Impedance ($Z$) is the ratio of voltage ($U$) and current ($I$) at a given frequency ($f$).

## 3. RESULTS

The results obtained from the electrochemical impedance measurements are presented in Figures 6, 7, and 8. For each membrane studied, the data are displayed using both the complex Nyquist plot (real versus imaginary parts of the impedance, Re vs Im; Figure 6) and the polar Bode plot (frequency ($f$) versus impedance magnitude (|z|) or phase angle ($\angle\varphi$); Figures 7 and 8, respectively). The Nyquist plots of PLFE and POPC/POPS show compressed semicircles, which could be attributed to the sample's chemical heterogeneity.[37] The magnitude of the impedance (|z|) for all membranes examined shows a sigmoidal change with frequency (Figure 7). Similar sigmoidal profiles were previously reported for DPPC monolayer coupled to octadecanethiol monolayer chemisorbed onto gold-coated solid surface.[38] However, the frequency dependence of |z| for PLFE is significantly different from those obtained from diester lipids and triblock copolymers (Figure 7). The $Z$ magnitude (|z|) of PLFE lipid membranes (Figure 7b) levels off at a frequency ~$10^2$ Hz, whereas |z| of other lipids levels off at a much higher frequency at ~$10^3$–$10^4$ Hz (Figure 7a,c,d). The profile of phase angle versus frequency for PLFE lipid membranes (Figure 8b) is also distinctly different from those seen from triblock copolymer, POPC, and POPC/POPS mixtures (Figure 8a,c,d). For triblock copolymer, POPC, and POPC/POPS mixtures, the plot of phase angle versus frequency displays an inverted bell shape, showing a minimal phase angle at ~50–100 Hz. In contrast, for PLFE lipid

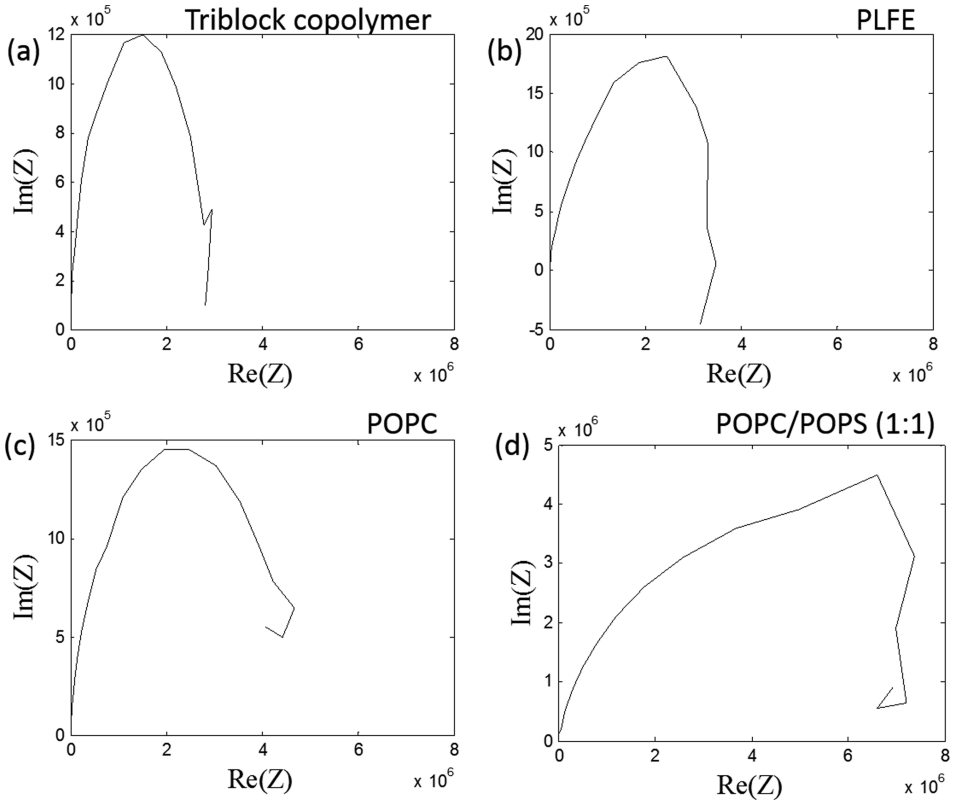


**Figure 6.** Revs-Im Nyquist plot of various planar membranes.

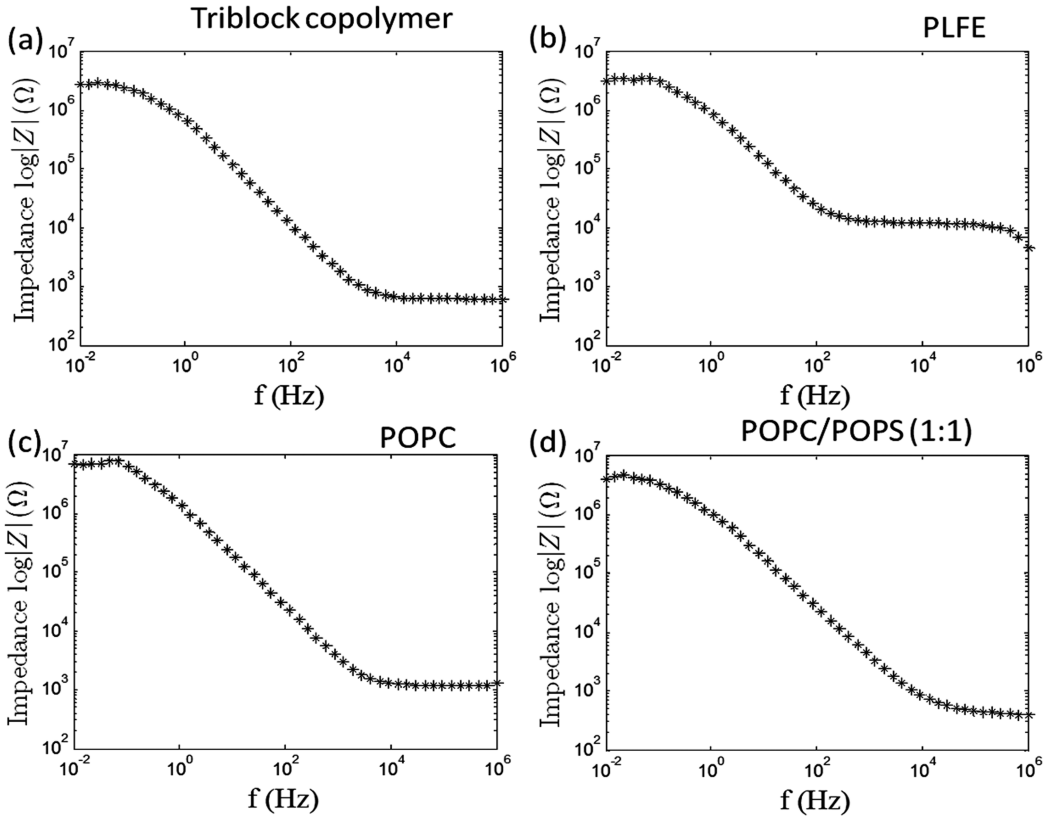


**Figure 7.** Frequency ($f$) vs impedance magnitude (|z|) in various planar membranes.

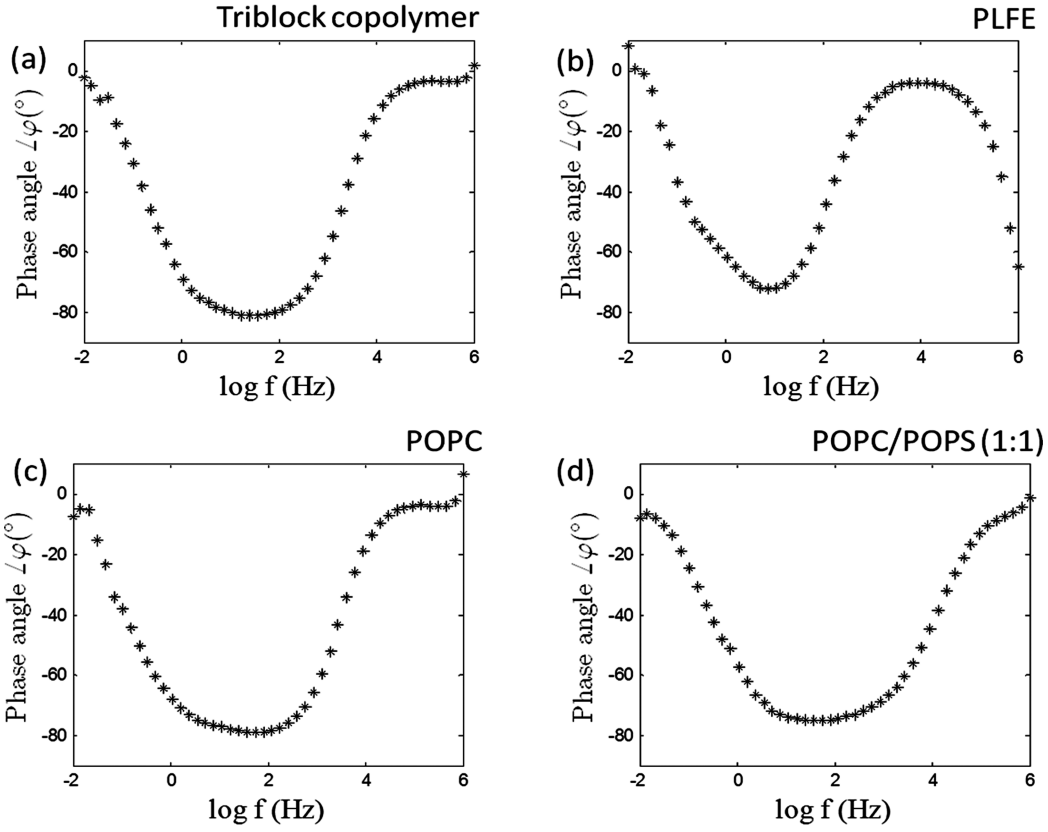


**Figure 8.** Frequency ($f$) vs phase angle ($\angle\varphi$) in various planar membranes.

membranes, the phase angle exhibits a biphasic change with frequency at 10 Hz and a sharp drop at ∼1 MHz.

The impedance equivalent circuits of various membranes (Figure 9) were obtained from the best fit of the experimental


dx.doi.org/10.1021/am502613x | ACS Appl. Mater. Interfaces 2014, 6, 12618−12628

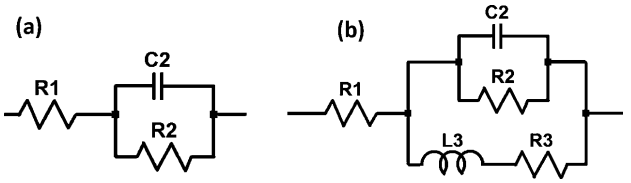


**Figure 9.** (a) Equivalent circuit of triblock copolymer, POPC or POPC/POPS planar membranes: R1+C2//R2; (b) equivalent circuit of PLFE planar membranes: R1+C2//R2//(L3+R3). R1 is the resistance of the electrolyte.

EIS data (Figures 6–8). The impedance of both triblock copolymer membranes and diester lipid membranes ($Z_{cp\text{-}dl}$) can be best described by the equivalent circuit: $R_1 + C_2//R_2$ (Figure 9a), in good agreement with previous studies.[39,40] Specifically

$$Z_{cp-dl} = R_1 + \frac{1}{j\omega C_2 + \frac{1}{R_2}} \quad (1)$$

which can be converted to

$$Z_{cp-dl} = R_1 + \frac{R_2}{1 + (\omega C_2 R_2)^2} - j\frac{\omega C_2 R_2}{1 + (\omega C_2 R_2)^2} \quad (2)$$

where $\omega = f/2\pi$.

The impedance of PLFE lipid membranes ($Z_{PLFE}$), on the other hand, can be best described by the equivalent circuit R1+C2//R2//(L3+R3) (Figure 9b), which can be expressed as

$$Z_{PLFE} = R_1 + \frac{1}{j\omega C_2 + \frac{1}{R_2} + \frac{1}{j\omega L_3 + R_3}} \quad (3)$$

Equation 3 can be rewritten in the form

$$Z_{PLFE} = R_1 + \frac{R_2^2 R_3 + R_2 R_3^2 + \omega^2 R_2 L_3^2}{(R_2 + R_3 - \omega^2 C_2 R_2 L_3)^2 + \omega^2 (C_2 R_2 R_3 + L_3)^2} + j\omega\frac{R_2^2 L_3 - C_2 R_2^2(\omega^2 L_3^2 + R_3^2)}{(R_2 + R_3 - \omega^2 C_2 R_2 L_3)^2 + \omega^2 (C_2 R_2 R_3 + L_3)^2} \quad (4)$$

To understand the physical meaning of the equivalent circuit, it is useful to dissect a membrane system into a series of slabs with different dielectric properties (e.g., the bilayer region and the aqueous phase with the electrolyte).[41] In the equivalent circuit of the triblock copolymer and diester lipid membranes (Figure 9a), R1 can be assigned to the electrolyte, and C2 and R2 are related to the membrane. Using this equivalent circuit and the EIS data (e.g., Figures 6–8), we determined that the triblock copolymer membrane has a membrane capacitance (C2) of $(0.29 \pm 0.01) \times 10^{-6}$ F/cm$^2$ ($n$ = 14) and a membrane resistance (R2) of 7.99 ± 0.02 Ω cm$^2$ ($n$ = 14), and the POPC membrane has a membrane capacitance (C2) of $(1.89 \pm 0.22) \times 10^{-6}$ F/cm$^2$ ($n$ = 9) and a membrane resistance (R2) of 1104 ± 91 Ω cm$^2$ ($n$ = 9). For the triblock copolymer and diester lipid membranes, the resistance $R$ = R1 + R2 (Figure 9a). The capacitance and resistance values of POPC and triblock copolymers obtained from our new fluidic device (Table 1) are comparable to those previously reported for free-standing planar membranes on PDMS or Teflon thin films.[42−46] This consistency validates our new PDMS- and PCB-based fluidic membrane design.

Similarly, R1 in the equivalent circuit of the PLFE lipid membrane can be assigned to the electrolyte layer, and the other electrochemical parameters are related to the membrane itself. We found that the PLFE lipid membrane has a membrane resistance ($R$) of $4.90 \pm 0.12 \times 10^3$ Ω cm$^2$ ($n$ = 12), which is much higher than that seen in triblock copolymer, POPC, and POPC/POPS planar membranes (Table 1). This large resistance for PLFE suggests that, among the membranes examined in this study, PLFE free-standing planar membrane would be a better lipid matrix for studying channel proteins and trans-membrane events. We also determined the PLFE membrane capacitance (C2) to be $(0.16 \pm 0.02) \times 10^{-6}$ F/cm$^2$ ($n$ = 12) and the membrane inductance (L3) to be $(1.23 \pm 0.29) \times 10^{-2}$ H/cm ($n$ = 12) (Table 1). Here $n$ is the number of experimental trials. Note that, for PLFE lipid membranes, $R$ = R1+R2//R3 whereas R2//R3 = (R2 × R3)/(R2 + R3) (Figure 9b). Also, note that the measured result of the equivalent circuit has taken into account the impedance of the PDMS thin film and the impedance offset caused by the PCB board which can be considered as a dielectric material. The impedance data of the empty PDMS chamber (without the free-standing planar membranes but with the electrolyte) are presented in Supporting Information (Figures S3–S5). The capacitance of the free-standing membrane was determined by comparing the membrane sample with an empty chamber with only the electrolyte (91.6 nF) (as described in Supporting Information).

## 4. DISCUSSION

It has long been proposed that archaeal bipolar tetraether lipids are potentially useful biomaterials for technology applications.[47−50] This point was first made based on the fact that tetraether lipids are chemically stable compared to diesters and that tetraether lipids are the major lipid components (e.g., >90%) in the plasma membrane of thermoacidophilic archaea (such as *S. acidocaldarius*), which thrive at high temperatures (~65–90 °C) and acidic conditions (pH 2–3).[51,52] This point was further substantiated by studies of tetraether liposomes. Compared to diester liposomes, tetraether liposomes (in particular, PLFE liposomes) exhibit low solute permeability; high stability against autoclaving, detergents, and fusogenic compounds; tight and

**Table 1. Comparison of Dielectric Properties of Different Planar Membranes[a]**

| membrane system | membrane capacitance from this study (μF/cm$^2$) | membrane resistance from this study (Ω cm$^2$) | membrane inductance from this study ($10^{-2}$ H/cm) | membrane capacitance reported by others (μF/cm$^2$) | membrane resistance reported by others (Ω cm$^2$) | membrane inductance reported by others (H/cm) |
|---|---|---|---|---|---|---|
| Triblock copolymer | 0.29 ± 0.01 ($n$ = 14) | 7.99 ± 0.02 ($n$ = 14) | None | 0.27[33] | 10.8[33] | NA |
| PLFE | 0.16 ± 0.02 ($n$ = 12) | 4901 ± 120 ($n$ = 12) | 1.23 ± 0.29 ($n$ = 12) | NA | NA | NA |
| POPC | 1.89 ± 0.22 ($n$ = 9) | 1104 ± 91 ($n$ = 9) | None | 1.2;[44,45] 1.96[38] | 855 ± 490[45] | NA |
| POPC/POPS (molar ratio: 1:1) | 1.21 ± 0.17 ($n$ = 10) | 868 ± 121 ($n$ = 10) | None | NA | NA | NA |

[a]The errors are the standard deviations from the mean values. NA: not available.

rigid membrane packing; low enthalpy and volume changes associated with the phase transitions; low compressibility; and low relative volume fluctuations (reviewed[15,22,23]). Because tetraether liposomes have such remarkable stability and because they are not toxic to animals,[53,54] many studies have been devoted to use archaeal tetraether liposomes as carriers of therapeutic agents (e.g., refs 24,48).

Here we extended the study of PLFE tetraether lipids from liposomes to free-standing planar membranes. We showed that the intact PLFE lipids (a partially purified tetraether lipid fraction from *S. acidocaldarius*) can form free-standing planar membranes on micropores of PDMS thin films. This finding will expand the application scope of PLFE lipids. Planar lipid membranes interposed between two aqueous solutions have been widely used as an experimental model of biomembranes and a platform for technological applications such as water filtration, drug screening, and biosensing.[10,55,56] The major problem of traditional free-standing planar membranes has been their low stability. They are delicate and last for only several hours.[10] Because the stability of free-standing lipid membranes is known to increase with increasing membrane packing tightness[1] and because PLFE lipid membranes are extremely tightly packed (discussed earlier), PLFE free-standing planar membranes are expected to be much more stable than those made of diester lipids. In fact, Melikyan et al. previously showed that black lipid membranes made of hydrolyzed GDNT isolated from *S. acidocaldarius* displayed higher membrane tension (4.3 mN/m) than those made of diester lipids (1.0−2.4 mN/m).[57] Several previous studies showed that while bipolar tetraether liposomes are tightly packed, membrane bound proteins can still insert into the membranes and retain their enzyme activities or transport functions (reviewed[16,58]). It is thus conceivable that membrane proteins can also be reconstituted into a stable PLFE free-standing planar membrane for various applications such as high throughput drug screening, biosensing, and artificial photosynthesis.

In terms of studying trans-membrane events and developing new applications, PLFE free-standing planar membranes are more attractive than archaeal lipid-based planar membranes previously reported. Early work on free-standing archaeal lipid membranes used the hydrolytic fraction of GDNT (SI Figure S1),[57,59−62] which had the sugar and phosphate groups removed. The removal of those moieties eliminates the ability of tetraether lipids to form a hydrogen-bond network in the polar headgroup regions of the membrane, consequently lowering membrane stability. The electrochemical data of solid-supported (not free-standing) as well as free-standing planar membranes made of the main tetraether phospholipid (MPL) fraction from the archaeon *Thermoplasma acidophilum* have previously been reported.[63,64] However, solid-supported planar membranes do not lend free access to both sides of the membrane as free-standing planar membrane does, and MPL from *T. acidophilum* has fewer sugar moieties (thus lower hydrogen bonding capabilities) than PLFE from *S. acidocaldarius*.[64]

Of particular interest is also the current finding that PLFE free-standing planar membranes exhibit unusual dielectric properties, compared to the planar membranes composed of diester lipids or triblock copolymers. We showed that the equivalent circuit of PLFE lipid membrane is different from that of diester lipid or triblock copolymer membrane (Figure 9). PLFE lipid membrane displays inductance in addition to capacitance and resistance, whereas the other three membranes examined do not display any inductance component (Figure 9 and Table 1). Additionally, there is a sharp decrease in phase angle with frequency at ∼1 MHz for PLFE (Figure 8b), but this sharp decrease is not observed from the other three membranes examined (Figure 8a,c,d). The molecular basis of the above-mentioned differences in dielectric properties is not known. At present, we can only speculate that these differential effects arise from the differences in membrane structure and membrane physical property (e.g., membrane dipole). An in-depth biophysical study is required in order to provide a mechanistic understanding of why PLFE lipid membranes show different dielectric properties from diester lipid and triblock copolymer membranes.

The ability to form stable free-standing planar membranes makes PLFE lipids particularly attractive for applications in microfluidics platforms (e.g., artificial photosynthesis). However, in the case of artificial photosynthesis, a fluidic device with one planar membrane and two compartments has limited ability for massive production of energy from light via the membrane bound proteins bacteriorhodopsin and ATP synthase (mentioned in Introduction). To increase the efficiency of energy production from planar membrane-based artificial photosynthesis systems, one can decrease the area of the planar membranes over the pinholes or increase the number of individual planar membranes. Therefore, an integration of a large number of the basic photosynthesis reaction unit is necessary. However, if one of the membranes breaks, the reaction solution in the two separate chambers will be mixed. As a result, the products will be contaminated by the reactants. Therefore, the real time monitoring of the membrane integrity is essential for prolonging the operational lifetime of an artificial photosynthesis board. If one of the membranes is broken, the sensors will identify and block the broken unit to prevent any further cross contamination. To construct such devices, the complementary metal−oxide−semiconductor (CMOS) sensors could be employed because of their low noise and fast operational speed. The working frequency of CMOS sensors is around 1 MHz. Interestingly, PLFE's impedance also has an obvious phase shift at 1 MHz (Figure 8b), which makes PLFE particularly suitable for fabricating integrated microfluidic devices such as artificial photosynthesis chips.[65] In essence, the impedance property detected on PLFE lipid membranes can be used as a sensor to inspect in real time the working status of the free-standing planar membrane on the PDMS films of the microfluidic device.

The work described here can be extended to nanopores on PDMS thin films in microfluidics and eventually add new impetus to the use of microelectromechanical systems and lab-on-a-chip technology for biosensing, bioanalytical chemistry, and bioengineering.[66,67]

## CONCLUSIONS

In this study, using EIS, we demonstrated that PLFE archaeal tetraether lipids can form free-standing planar membranes on micropores of PDMS thin films in a home-built PCB-based fluidic device. The fabrication of the PDMS film and the fluidics is facilitated by the use of an S1813 sacrificial layer and oxygen plasma treatment. In comparison to the planar membranes of diester lipids (POPC and POPC/POPS) and triblock copolymers (PMOXA−PDMS−PMOXA) made by the same method and device, PLFE free-standing planar membrane exhibits unusual dielectric properties, showing an inductance component, a large membrane resistance, and a sharp drop in phase angle with input electrical signal frequency at ∼1 MHz. The large resistance suggests that, among the membranes examined, PLFE

free-standing planar membrane is a better lipid matrix for studying channel proteins and trans-membrane events. The presence of the inductance component and the sharp drop in phase angle can be developed as a sensor to monitor the PLFE membrane status in the fluidics platform. Based on our current knowledge of bipolar tetraether lipids and lipid vesicles, PLFE free-standing planar membranes situated in the PDMS- and PCB-based fluidics are expected to be stable and thus suitable for various applications such as high-throughput drug screening and artificial photosynthesis.

## ■ ASSOCIATED CONTENT

### Supporting Information

Chemical structures of the lipids and triblock copolymers that were used to make free-standing planar membranes; impedance data obtained from the empty PDMS chamber. This material is available free of charge via the Internet at http://pubs.acs.org.

## ■ AUTHOR INFORMATION

### Corresponding Authors

*E-mail: zhoug@coe.drexel.edu.
*E-mail: pchong02@temple.edu.

### Notes

The authors declare no competing financial interest.

## ■ ACKNOWLEDGMENTS

The authors thank the support from National Science Foundation on award numbers CMMI-1141815, CMMI-1141830, CMMI-1266306, and DMR-1105277. The authors would also like to thank Huy Vo and Microfabrication Laboratory at Johns Hopkins University for using their equipment, and Youngbok Kang and Chris Dennison for their technical assistance, as well as the support from Centralized Research Facilities at Drexel University.

## ■ ABBREVIATIONS

ATP, adenosine triphosphate; BR, bacteriorhodopsin; CMOS, complementary metal−oxide−semiconductor; EIS, electrochemical impedance spectroscopy; GDNT, glycerol dialkylcaldidtol tetraether; GDGT, glycerol dialkylglycerol tetraether; MPL, main tetraether phospholipid fraction; PCB, printed circuit board; PDMS, polydimethylsiloxane; PLFE, the polar lipid fraction E; PMOXA−PDMS−PMOXA, poly(2-methyloxazoline)-*block*-poly(dimethylsiloxane)-*block*-poly(2-methyloxazoline); POPC, 1-palmitoyl-2-oleoyl-*sn*-glycero-3-phosphocholine; POPS, 1-palmitoyl-2-oleoyl-*sn*-glycero-3-phosphoserine

## ■ REFERENCES

(1) Malmstadt, N.; Nash, M. A.; Purnell, R. F.; Schmidt, J. J. Automated Formation of Lipid-Bilayer Membranes in a Microfluidic Device. *Nano Lett.* **2006**, *6*, 1961−1965.
(2) Choi, H.-J.; Montemagno, C. D. Biosynthesis within a Bubble Architecture. *Nanotechnology* **2006**, *17*, 2198−2202.
(3) Wendell, D.; Todd, J.; Montemagno, C. Artificial Photosynthesis in Ranaspumin-2 Based Foam. *Nano Lett.* **2010**, *10*, 3231−3236.
(4) Kongsuphol, P.; Fang, K. B.; Ding, Z. Lipid Bilayer Technologies in Ion Channel Recordings and their Potential in Drug Screening Assay. *Sens. Actuators* **2013**, *B185*, 530−542.
(5) Nardin, C.; Hirt, T.; Leukel, J.; Meier, W. Polymerized ABA Triblock Copolymer Vesicles. *Langmuir* **2000**, *16*, 1035−1041.
(6) Choi, H. J.; Germain, J.; Montemagno, C. D. Effects of Different Reconstitution Procedures on Membrane Protein Activities in Proteopolymersomes. *Nanotechnology* **2006**, *17*, 1825−1830.
(7) Roman-Leshkov, Y.; Barrett, C. J.; Liu, Z. Y.; Dumesic, J. A. Production of Dimethylfuran for Liquid Fuels from Biomass-Derived Carbohydrates. *Nature* **2007**, *447*, 982−985.
(8) Schmidt, C.; Mayer, M.; Vogel, H. A Chip-Based Biosensor for the Functional Analysis of Single Ion Channels. *Angew. Chem. Int.* **2000**, *39*, 3137−3140.
(9) Cheng, Y.; Bushby, R. J.; Evans, S. D.; Knowles, P. F.; Miles, R. E.; Ogier, S. D. Single Ion Channel Sensitivity in Suspended Bilayers on Micromachined Supports. *Langmuir* **2001**, *17*, 1240−1242.
(10) Tien, H. T.; Ottova, A. L. The Lipid Bilayer Concept and its Experimental Realization: From Soap Bubbles, Kitchen Sink, to Bilayer Lipid Membranes. *J. Membr. Sci.* **2001**, *189*, 83−117.
(11) Romer, W.; Steinem, C. Impedance Analysis and Single-Channel Recordings on Nano-Black Lipid Membranes Based on Porous Alumina. *Biophys. J.* **2004**, *86*, 955−965.
(12) Han, X.; Studer, A.; Sehr, H.; Geissbuhler, I.; Di Berardino, M.; Winkler, F. K.; Tiefenauer, L. X. Nanopore Arrays for Stable and Functional Free-Standing Lipid Bilayers. *Adv. Mater.* **2007**, *19*, 4466−4470.
(13) Studer, A.; Tiefenauer, L. X. Stable Planar Lipid Bilayers in Nanopores. *Eur. Cells Mater.* **2007**, *14* (Suppl. 3), 33.
(14) Brock, T. D.; Brock, K. M.; Belly, R. T.; Weiss, R. L. Sulfolobus: a New Genus of Sulfur-Oxidizing Bacteria Living at Low pH and High Temperature. *Archiv. Mikrobiologie* **1972**, *84*, 54−68.
(15) Chong, P. L.-G. Archaebacterial Bipolar Tetraether Lipids: Physico-Chemical and Membrane Properties. *Chem. Phys. Lipids* **2010**, *163*, 253−265.
(16) Jacquemet, A.; Barbeau, J.; Lemiègre, L.; Benvegnu, T. Archaeal Tetraether Bipolar Lipids: Structures, Functions and Applications. *Biochimie* **2009**, *91*, 711−717.
(17) Lo, S. L.; Chang, E. L. Purification and Characterization of a Liposomal-Forming Tetraether Lipid Fraction. *Biochem. Biophys. Res. Commun.* **1990**, *167*, 238−243.
(18) Sugai, A.; Sakuma, R.; Fukuda, I.; Kurosawa, N.; Itoh, Y. H.; Kon, K.; Ando, S.; Itoh, T. The Structure of the Core Polyol of the Ether Lipids from *Sulfolobus acidocaldarius*. *Lipids* **1995**, *30*, 339−344.
(19) Jeworrek, C.; Evers, F.; Erlkamp, M.; Grobelny, S.; Tolan, M.; Chong, P. L.-G.; Winter, R. Structure and Phase Behavior of Archaeal Lipid Monolayers. *Langmuir* **2011**, *27*, 13113−13121.
(20) Bagatolli, L. A.; Gratton, E.; Khan, T. K.; Chong, P. L.-G. Two-Photon Fluorescence Microscopy Studies of Bipolar Tetraether Giant Liposomes from Thermoacidophilic Archaebacteria *Sulfolobus acidocaldarius*. *Biophys. J.* **2000**, *79*, 416−425.
(21) Chong, P. L.-G.; Zein, M.; Khan, T. K.; Winter, R. Structure and Conformation of Bipolar Tetraether Lipid Membranes Derived from Thermoacidophilic Archaeon *Sulfolobus acidocaldarius* as Revealed by Small-Angle X-Ray Scattering and High Pressure FT-IR Spectroscopy. *J. Phys. Chem. B* **2003**, *107*, 8694−8700.
(22) Chong, P. L.-G.; Ayesa, U.; Daswani, V. P.; Hur, E. C. On Physical Properties of Tetraether Lipid Membranes: Effects of Cyclopentane Rings. *Archaea* **2012**, DOI: 10.1155/2012/138439.
(23) Gliozzi, A.; Relini, A.; Chong, P. L.-G. Structure and Permeability Properties of Biomimetic Membranes of Bolaform Archaeal Tetraether Lipids. *J. Membr. Sci.* **2002**, *206*, 131−147.
(24) Sprott, G. D.; Patel, G. B.; Krishnan, L. Archaeobacterial Ether Lipid Liposomes as Vaccine Adjuvants. *Methods Enzymol.* **2003**, *373*, 155−172.
(25) Zhai, Y.; Chong, P. L.-G.; Taylor, L. J.-A.; Erlkamp, M.; Grobelny, S.; Czeslik, C.; Watkins, E.; Winter, R. Physical Properties of Archaeal Tetraether Lipid Membranes as Revealed by Differential Scanning and Pressure Perturbation Calorimetry, Molecular Acoustics, and Neutron Reflectometry: Effects of Pressure and Cell Growth Temperature. *Langmuir* **2012**, *28*, 5211−5217.
(26) Moffitt, M.; Khougaz, K.; Eisenberg, A. Micellization of Ionic Block Copolymers. *Acc. Chem. Res.* **1996**, *29*, 95−102.
(27) McDonald, J. C.; Whitesides, G. M. Poly(dimethylsiloxane) as a Material for Fabricating Microfluidic Devices. *Acc. Chem. Res.* **2002**, *35*, 491−499.

(28) Sodunkea, T. R.; Turnerb, K. K.; Caldwellb, S. A.; McBridec, K. W.; Reginatob, M. J.; Noh, H. Micropatterns of Matrigel for Three-Dimensional Epithelial Cultures. *Biomaterials* **2007**, *28*, 4006−4016.
(29) Walther, F.; Davydovskaya, P.; Zürcher, S.; Kaiser, M.; Herberg, H.; Gigler, A. M.; Stark, R. W. Stability of the Hydrophilic Behavior of Oxygen Plasma Activated SU-8. *J. Micromech. Microeng.* **2007**, *17*, 524−531.
(30) Cai, D. K.; Neyer, A. Polysiloxane Based Flexible Electrical Optical Circuits Board. *Microelectron. Eng.* **2010**, *87*, 2268−2274.
(31) Welch, D.; Christen, J. B. Seamless Integration of CMOS and Microfluidics using Flip Chip Bonding. *J. Micromech. Microeng.* **2013**, DOI: 10.1088/0960-1317/23/3/035009.
(32) Jang, L.-S.; Wu, C.-C.; Liu, C.-F. Fabrication of Microfluidic Devices for Packaging CMOS MEMS Impedance Sensors. *Microfluid. Nanofluid.* **2009**, *7*, 869−875.
(33) Choi, H. J.; Brooks, E.; Montemagno, C. D. Synthesis and Characterization of Nanoscale Biomimetic Polymer Vesicles and Polymer Membranes for Bioelectronic Applications. *Nanotechnology* **2005**, *16*, 143−149.
(34) Lei, S. B.; Tero, R.; Misawa, N.; Yamamura, S.; Wan, L. J.; Urisu, T. AFM Characterization of Gramicidin-A in Tethered Lipid Membrane on Silicon Surface. *Chem. Phys. Lett.* **2006**, *429*, 244−249.
(35) Abdelghani, A.; Jacquin, C.; Huber, M.; Deutschmann, R.; Sackmann, E. Supported Lipid Membrane on Semiconductor Electrode. *Mater. Chem. Phys.* **2001**, *70*, 187−190.
(36) Nardin, C.; Winterhalter, M.; Meier, W. Giant Free-Standing ABA Triblock Copolymer Membranes. *Langmuir* **2000**, *16*, 7708−7712.
(37) O'Rourke, M.; Duffy, N.; Marco, R.; Potter, I. Electrochemical Impedance Spectroscopy–a Simple Method for the Characterization of Polymer Inclusion Membranes Containing Aliquat 336. *Membranes* **2011**, *1*, 132−148.
(38) Steinem, C.; Janshoff, A.; Ulrich, W.-P.; Sieber, M.; Galla, H.-J. Impedance Analysis of Supported Lipid Bilayer Membranes: A Scrutiny of Different Preparation Techniques. *Biochim. Biophys. Acta* **1996**, *1279*, 169−180.
(39) Gritsch, S.; Nollert, P.; Jahnig, F.; Sackmann, E. Impedance Spectroscopy of Porin and Gramicidin Pores Reconstituted into Supported Lipid Bilayers on Indium-Tin-Oxide Electrodes. *Langmuir* **1998**, *14*, 3118−3125.
(40) Naumann, R.; Baumgart, T.; Graber, P.; Jonczyk, A.; Offenhausser, A.; Knoll, W. Proton Transport through a Peptide-Tethered Bilayer Lipid Membrane by the $H^+$-ATP Synthase from Chloroplasts Measured by Impedance Spectroscopy. *Biosens. Bioelectron.* **2002**, *17*, 25−34.
(41) Becucci, L.; Martinuzzi, S.; Monetti, E.; Mercatelli, R.; Quercioli, F.; Battistel, D.; Guidelli, R. Electrochemical Impedance Spectroscopy and Fluorescence Lifetime Imaging of Lipid Mixtures Self-Assembled on Mercury. *Soft Matter* **2010**, *6*, 2733−2741.
(42) Faiß, S.; Kastl, K.; Janshoff, A.; Steinem, C. Formation of Irreversibly Bound Annexin A1 Protein Domains on POPC/POPS Solid Supported Membranes. *Biochim. Biophys. Acta* **2008**, *1778*, 1601−1610.
(43) Kastl, K.; Menke, M.; Lüthgens, E.; Faiß, S.; Gerke, V.; Janshoff, A.; Steinem, C. Partially Reversible Adsorption of Annexin A1 on POPC/POPS Bilayers Investigated by QCM Measurements, SFM, and DMC Simulations. *ChemBioChem* **2006**, *7*, 106−115.
(44) Lundgren, A.; Hedlund, J.; Andersson, O.; Branden, M.; Kunze, A.; Elwing, H.; Hook, F. Resonance-Mode Electrochemical Impedance Measurements of Silicon Dioxide Supported Lipid Bilayer Formation and Ion Channel Mediated Charge Transport. *Anal. Chem.* **2011**, *83*, 7800−7806.
(45) Lin, J.; Szymanski, J.; Searson, P. C.; Hristova, K. Electrically Addressable, Biologically Relevant Surface-Supported Bilayers. *Langmuir* **2010**, *26*, 12054−12059.
(46) Morigaki, K.; Tawa, K. Vesicle Fusion Studied by Surface Plasmon Resonance and Surface Plasmon Fluorescence Spectroscopy. *Biophys. J.* **2006**, *91*, 1380−1387.
(47) Gambacorta, A.; Gliozzi, A.; De Rosa, M. Archaeal Lipids and their Biotechnological Applications. *World J. Microbiol. Biotechnol.* **1995**, *11*, 115−132.
(48) Patel, G. B.; Sprott, G. D. Archaeobacterial Ether Lipid Liposomes (Archaeosomes) as Novel Vaccine and Drug Delivery Systems. *Crit. Rev. Biotechnol.* **1999**, *19*, 317−357.
(49) Schiraldi, C.; Giuliano, M.; De Rosa, M. Perspectives on Biotechnological Applications of Archaea. *Archaea* **2002**, *1*, 75−86.
(50) Benvegnu, T.; Lemiègre, L.; Cammas-Marion, S. Archaeal Lipids: Innovative Materials for Biotechnological Applications. *Eur. J. Org. Chem.* **2008**, *2008*, 4725−4744.
(51) Kates, M. In *The Archaebacteria: Biochemistry and Biotechnology*; Danson, M. J., Hough, D. W., Lunt, G. G., Eds.; Portland Press: London, 1992; pp 51−72.
(52) Langworthy, T. A.; Pond, J. L. Membranes and Lipids of Thermophiles. In *Thermophiles: General, Molecular, and Applied Microbiology*; Brock,T. D., Ed.; John Wiley & Sons: New York, 1986; pp 107−134.
(53) Freisleben, H.-J.; Bormann, J.; Litzinger, D. C.; Lehr, F.; Rudolph, P.; Schatton, M.; Huang, L. Toxicity and Biodistribution of Liposomes of the Main Phospholipid from the Archaebacterium *Thermoplasma acidophilum*. *J. Liposome Res.* **1995**, *5*, 215−223.
(54) Patel, G. B.; Ponce, A.; Zhou, H.; Chen, W. Safety of Intranasally Administered Archaeal Lipid Mucosal Vaccine Adjuvant and Delivery (AMVAD) Vaccine in Mice. *Int. J. Toxicol.* **2008**, *27*, 329−339.
(55) Kaufmana, Y.; Grinberg, S.; Linder, C.; Heldmand, E.; Gilrone, J.; Shenf, Y.; Kumar, M.; Lammertinkg, R. G. H.; Freger, V. Towards Supported Bolaamphiphile Membranes for Water filtration: Roles of Lipid and Substrate. *J. Membr. Sci.* **2014**, *457*, 50−61.
(56) Bally, M.; Bailey, K.; Sugihara, K.; Grieshaber, D.; Voros, J.; Stadler, B. Liposomes and Lipid Bilayer Arrays towards Biosensing Applications. *Small* **2010**, *6*, 2481−2497.
(57) Melikyan, G. B.; Matinyan, N. S.; Kocharov, S. L.; Arakelian, V. B.; Prangishvili, D. A.; Nadareishvili, K. G. Electromechanical Stability of Planar Lipid Membranes from Bipolar Lipids of the Thermoacidophilic Archaebacterium *Sulfolobus acidocaldarius*. *Biochim. Biophys. Acta* **1991**, *1068*, 245−248.
(58) Chong, P. L.-G. In *Thermophiles*; Robb, F., Antranikian, G., Grogan, D., and Driessen, A., Eds.; CRC Press: Boca Raton, FL, 2008; Chapter 6, pp 73−95.
(59) Fittabile, L.; Robello, M.; Relini, A.; De Rosa, M.; Gliozzi, A. Organization of Monolayer-Formed Membranes Made from Archaeal Ether Lipids. *Thin Solid Films* **1996**, *284−285*, 735−738.
(60) Gliozzi, A.; Robello, M.; Relini, A.; Accardo, G. Asymmetric Black Membranes Formed by One Monolayer of Bipolar Lipids at the Air/Water Interface. *Biochim. Biophys. Acta* **1993**, *1189*, 96−100.
(61) Gliozzi, A.; Rolandi, R.; De Rosa, M.; Gambacorta, A. Monolayer Black Membranes from Bipolar Lipids of Archaebacteria and their Temperature-Induced Structural Changes. *J. Membr. Biol.* **1983**, *75*, 45−56.
(62) Gliozzi, A.; Rolandi, R.; De Rosa, M.; Gambacorta, A. Artificial Black Membranes from Bipolar Lipids of Thermophilic Archaebacteria. *Biophys. J.* **1982**, *37*, 563−566.
(63) Gufler, P. C.; Pum, D.; Sleytr, U. B.; Schuster, B. Highly Robust Lipid Membranes on Crystalline S-Layer Supports Investigated by Electrochemical Impedance Spectroscopy. *Biochim. Biophys. Acta* **2004**, *1661*, 154−165.
(64) Stern, J.; Freisleben, H.-J.; Janku, S.; Ring, K. Black Lipid Membranes of Tetraether Lipids from *Thermoplasma acidophilum*. *Biochim. Biophys. Acta* **1992**, *1128*, 227−236.
(65) Lee, J. S.; Lee, S. H.; Kim, J. H.; Park, C. B. Artificial Photosynthesis on a Chip: Microfluidic Cofactor Regeneration and Photoenzymatic Synthesis Under Visible Light. *Lab Chip* **2011**, *11*, 2309−2311.
(66) Ziaie, B.; Baldi, A.; Lei, M.; Gu, Y.; Siegel, R. A. Hard and Soft Micromachining for BioMEMS: Review of Techniques and Examples of Applications in Microfluidics and Drug Delivery. *Adv. Drug Delivery Rev.* **2004**, *56*, 145−172.

(67) West, J.; Becker, M.; Tombrink, S.; Manz, A. Micro Total Analysis Systems: Latest Achievements. *Anal. Chem.* **2008**, *80*, 4403−4419.